J. metamorphic Geol., 2004, **22,** 427–442 doi:10.1111/j.1525-1314.2004.00524.x

High-Si phengite records the time of greenschist facies overprinting: implications for models suggesting mega-detachments in the Aegean Sea

M. BRÖCKER[1], D. BIELING[1], B. HACKER[2] AND P. GANS[2]
[1]*Institut für Mineralogie, Zentrallaboratorium für Geochronologie, Corrensstr. 24, 48149 Münster, Germany (brocker@nwz.uni-muenster.de)*
[2]*Department of Geological Sciences and Institute for Crustal Studies, University of California, Santa Barbara, CA 93106-9630, USA*

ABSTRACT In the lower main unit of the Attic-Cycladic crystalline belt (Greece), white mica geochronology (Rb–Sr, K–Ar, ^{40}Ar–^{39}Ar) has established the timing of at least two metamorphic events: well-preserved high-pressure/low-temperature (HP/LT) rocks yielded Eocene ages (*c.* 53–40 Ma) and their greenschist facies counterparts provided Oligocene–Miocene dates (*c.* 25–18 Ma). Marbles from Tinos Island contain high-Si phengite with Rb–Sr (phengite–calcite) and ^{40}Ar–^{39}Ar white mica ages between 41 and 24 Ma. All Ar age spectra are disturbed and ^{40}Ar–^{39}Ar total fusion ages generally are 3–6 Ma older than corresponding Rb–Sr ages. Due to the polymetamorphic history, we consider inheritance from the HP stage as the most likely cause for the complex Ar age spectra and the older ^{40}Ar–^{39}Ar dates. This concept also suggests that the Rb–Sr system is more sensitive to modification during overprinting than the Ar isotope system, because resetting of the Sr isotope system can be accomplished more quickly by Sr exchange with other Ca-rich phases, whereas lack of pervasive deformation and/or restricted availability of synmetamorphic fluids has favoured partial inheritance of the Ar isotope system. On Tinos, the lowermost part of the metamorphic succession has experienced a pervasive greenschist facies overprint. Si-rich phengite from marbles representing this lithostratigraphic level yielded Rb–Sr ages of *c.* 24 Ma. If the earlier metamorphic history is not taken into account, such data sets may lead to the erroneous conclusion of Miocene HP metamorphism. This study indicates that this phengite experienced pervasive rejuvenation of the Rb–Sr isotope system during overprinting, without significant changes in Si content, due to bulk-compositional constraints. This leads to the conclusion that in the absence of critical mineral assemblages the Si value of phengite is not a reliable indicator for metamorphic pressures in impure marbles. Recent studies have reported large displacements (> 100 km) for detachment faults in the Aegean Sea. A critical parameter for such models is the age of HP metamorphism as deduced from white mica dating in the basal units of the Cyclades. We question the underlying idea of Miocene HP metamorphism and suggest, instead, that this age constrains the timing of the greenschist facies overprint and that the existence of mega-detachments in the study area requires further investigation.

Key words: Aegean Sea; ^{40}Ar–^{39}Ar dating; high-Si phengite; marbles; mega-detachments; Rb–Sr dating.

INTRODUCTION

In the lower main unit of the Attic-Cycladic crystalline belt (ACCB) (Greece), white mica geochronology (Rb–Sr, K–Ar, ^{40}Ar–^{39}Ar) has established time constraints for at least two metamorphic events during the Tertiary. Well-preserved high-pressure/low-temperature (HP/LT) rocks have yielded Eocene ages (*c.* 53–40 Ma) and their greenschist facies counterparts mostly have provided Oligocene–Miocene ages (*c.* 25–18 Ma) (e.g. Altherr *et al.*, 1979, 1982; Wijbrans & McDougall, 1986, 1988; Wijbrans *et al.*, 1990; Bröcker *et al.*, 1993; Bröcker & Franz, 1998; Tomaschek *et al.*, 2003). Previous studies have indicated that the geochronological record of high-Si phengite may not correspond to the HP stage but to the subsequent greenschist facies overprint. This hypothesis is based on the observation that the range in Si contents and the modal proportions of phengite with a specific Si value in many cases do not differ significantly between the HP rocks and the pervasively overprinted greenschists (Bröcker *et al.*, 1993; Bröcker & Franz, 1998). Thus, the major-element compositions of phengite cannot be used to distinguish between samples providing Eocene or Oligocene/Miocene ages (Bröcker *et al.*, 1993; Bröcker & Franz, 1998). The possibility that the barometric information and the geochronological record might be decoupled is of general importance for the interpretation of phengite dates from polymetamorphic terranes and has significant implications for understanding the regional geology of the study area. For example, recent studies have reported large displacements (> 100 km)

for detachment faults of the Aegean region (Ring *et al.*, 2001; Ring & Reischmann, 2002). A critical aspect for these models is the age of the HP metamorphism, as deduced from ^{40}Ar–^{39}Ar and Rb–Sr dating of high-Si phengite.

To look in more detail into the relationship between Si content and white mica ages we have studied calcite marbles from the island of Tinos (Figs 1 and 2). As also observed on other islands in the study area (e.g. Syros, Sifnos), there is a gradient in the preservation of HP rocks, which are best preserved in the upper part of the metamorphic succession. Towards the base, the degree of retrogression increases and pervasively overprinted greenschist facies sequences predominate at lower lithostratigraphic levels. The marbles were selected because they often contain white mica populations consisting largely of Si-rich phengite. Therefore, it can be expected that the relationship between radiometric age and Si content will not significantly be obscured by complexities caused by the presence of mixed age populations.

By application of phengite geochronology (Rb–Sr, ^{40}Ar–^{39}Ar) and electron microprobe (EMP) analysis, the following questions are addressed in this paper: What is the relationship between Si contents and ages of white mica? Which metamorphic episode is dated: the blueschist facies event or the greenschist facies overprint? Furthermore, we present a set of hypotheses to account for the difference between apparent ^{40}Ar–^{39}Ar and Rb–Sr ages for the same phengite and discuss the potential risks to tectonic interpretation in polymetamorphic terranes that can arise from uncritical linkage of phengite-based pressures and ages.

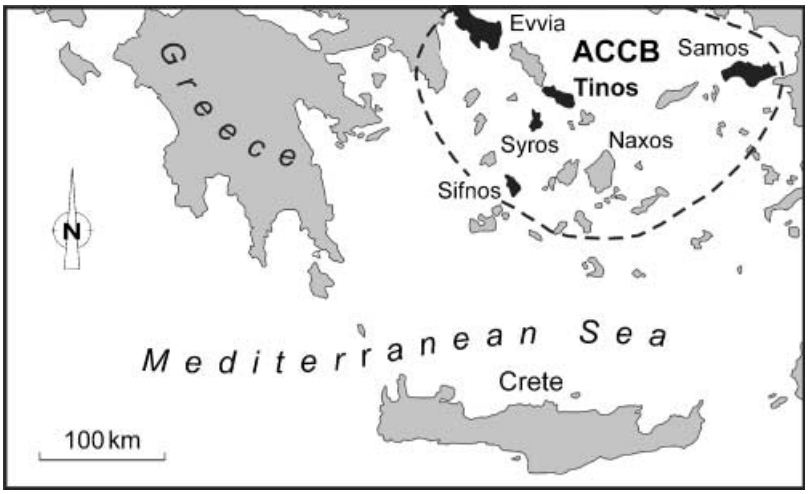

Fig. 1. General map of the Cyclades, showing the location of the study area and the Attic-Cycladic crystalline belt.

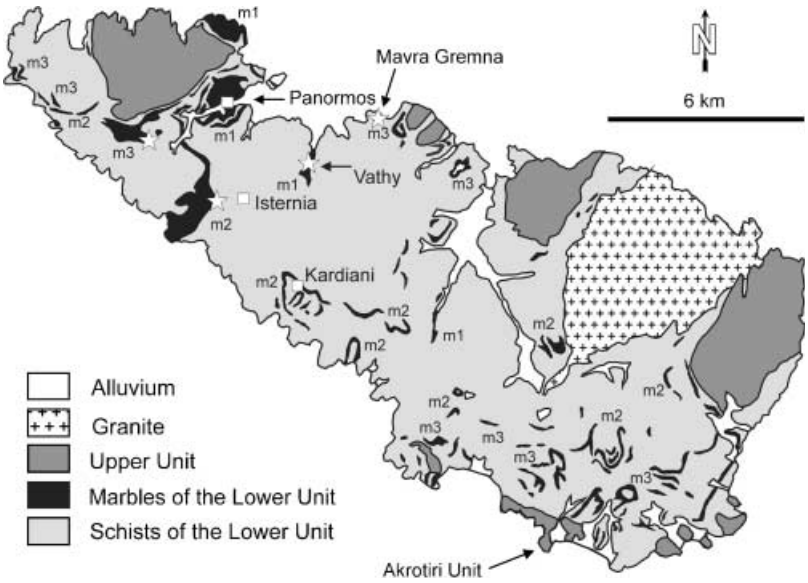

Fig. 2. Simplified geological map of Tinos (modified after Melidonis, 1980). Open squares indicate villages; stars indicate sample sites.

GEOLOGICAL SETTING

The ACCB is a polymetamorphic terrane that belongs to the Alpine-type Hellenic orogen in the Aegean region. The metamorphic evolution of its lower main unit (=Cycladic blueschist unit, CBU) comprises two major events that occurred under different baric conditions: (1) Cretaceous to Eocene HP/LT metamorphism and (2) a subsequent greenschist to amphibolite facies overprint (e.g. Dürr, 1986; Okrusch & Bröcker, 1990).

On Tinos (Fig. 2) a representative fragment of the ACCB is exposed in at least three tectonic units (cf. Melidonis, 1980; Bröcker & Franz, 2000). The two tectonic subunits occupying the highest structural levels (Akrotiri unit and upper unit) belong to the upper main unit of the ACCB, which was not affected by HP metamorphism. The amphibolite facies rocks of the *Akrotiri Unit* yielded K–Ar hornblende ages of *c*. 67 Ma (Patzak *et al*., 1994). The structurally underlying *Upper Unit* (≤250 m thick) consists of a disrupted meta-ophiolite sequence of unknown protolith age, composed of serpentinites, ophicalcites, metagabbros and phyllitic rocks (Katzir *et al*., 1996). Geochronological data are available only for the greenschist facies phyllites, which yielded Rb–Sr dates (phengite–whole-rock) between 92–21 Ma (Bröcker & Franz, 1998). Most of the island belongs to the *Blue-Schist–Greenschist Unit* (BGU) (about 1250–1800 m in thickness; in the local literature also referred to as *Lower Unit* or *Intermediate Unit*). The BGU belongs to the lower main unit of the ACCB and has experienced eclogite- to epidote–blueschist facies metamorphism ($T = 450$–500 °C, $P > 12$ kbar) and a greenschist facies overprint ($T = 450$–500 °C, $P = 4$–7 kbar) during the Tertiary (e.g. Bröcker *et al*., 1993). HP metamorphism may have started as early as the Cretaceous (*c*. 80 Ma; Bröcker & Enders, 1999; for a contrasting view see Tomaschek *et al*., 2003). Marbles, calcschists, siliciclastic meta-sediments, cherts, basic and acidic metavolcanic rocks are the principal rock types (Melidonis, 1980; Bröcker, 1990a). Remnants of eclogite- and blueschist facies rocks were recognized at many places on the island, but pervasively overprinted rocks with greenschist facies mineralogies are more common (e.g. Melidonis, 1980; Bröcker, 1990a,b). HP rocks are best preserved in the upper parts of the metamorphic succession. Towards the base, the degree of greenschist facies overprinting increases. The status of the lowermost parts of the metamorphic succession, which consists mainly of dolomite marbles and minor phyllites (Fig. 3), is controversial. According to Avigad & Garfunkel (1989), these rocks represent a para-authochthonous *Basal Unit*, which is separated from the structurally higher sequences of the BGU by a thrust fault. The inferred peak metamorphic conditions in this presumed tectonic subunit were considered to be low-grade greenschist facies (Avigad & Garfunkel, 1989). This interpretation was recently challenged by Bröcker & Franz (submitted), who suggested blueschist facies metamorphism for the dolomite–phyllite sequence. According to these authors the basal sequences are an integral part of the BGU, as originally proposed by Melidonis (1980).

FIELD RELATIONSHIP AND SAMPLE DESCRIPTION

Melidonis (1980) showed that the BGU can be subdivided roughly by three mappable marble sequences

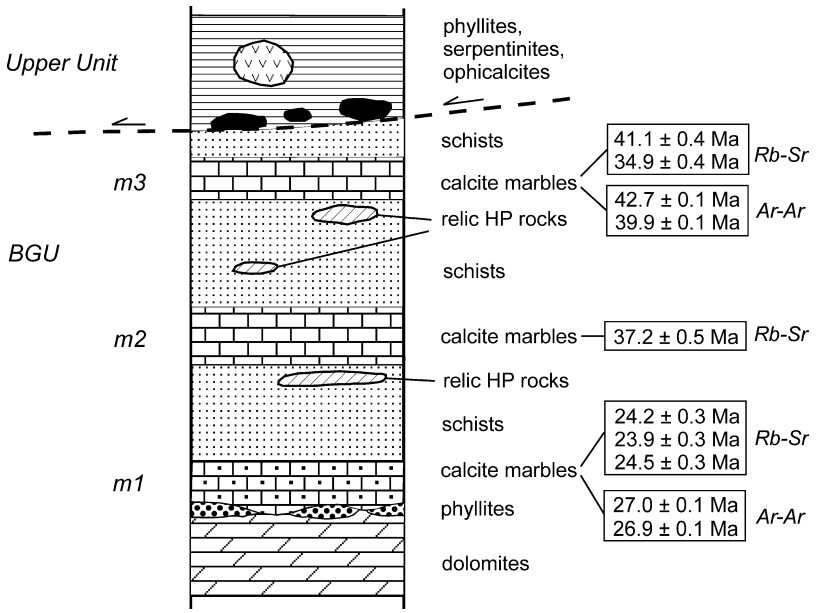

Fig. 3. Schematic columnar section of the metamorphic succession in NW Tinos (modified after Melidonis, 1980; Bröcker, 1990a).

(labelled m3, m2 and m1 from top to bottom), which locally are intercalated with clastic metasediments or metabasic rocks (Figs 2 & 3). This lithological field criterion is best applicable in NW Tinos, where the thickness of the marble units mostly is in the order of tens of metres (*c.* 50–150 m). In other parts of the island, the marbles are much thinner and the classification of distinct horizons as m3, m2 or m1 is more difficult, due to the common interlayering of relatively thin marbles with other lithologies. The studied samples were collected in NW Tinos (Fig. 3), where the marble sequences can clearly be assigned to distinct lithostratigraphic levels (Melidonis, 1980; Bröcker, 1990a). The uppermost m3 sequence was studied at two places (Marlas region, Mavra Gremna) about 6 km apart (Fig. 2). At both places, the meta-carbonates are underlain by clastic metasediments and a meta-conglomerate or meta-debris flow with subangular to rounded clasts (< 20 cm), composed of marbles and minor metabasic rocks (Bröcker, 1990a; this study). The studied sample from the intermediate marble sequence (m2) was collected near Isternia (Fig. 2), directly above one of the best-preserved occurrences of blueschist facies rocks on Tinos (e.g. Bröcker *et al.*, 1993; Breeding *et al.*, 2003). The m1 marbles are best exposed in the Panormos and Vathy areas (Fig. 2). Around Panormos, the carbonate sequence consists of calcite-rich marbles (*c.* 50 m), typically intercalated with thin bands of quartzite (mostly < 5 cm; rarely up to 20 cm), which are underlain by a thin phyllite horizon (1–2 m) and dolomites (*c.* 100 m) (Avigad & Garfunkel, 1989; Matthews *et al.*, 1999). Originally, this succession was assigned to the BGU (Melidonis, 1980). Subsequently, Avigad & Garfunkel (1989) suggested that the lowermost parts of the m1 sequence (consisting of dolomites and minor phyllites) represent a distinct tectonic subunit with a metamorphic history that is different to the overlying rock sequences. We follow Melidonis (1980) and regard the Panormos section as integral part of the BGU. For the questions addressed in this paper, it is worth emphasizing that the studied m1 samples from the Vathy area (Fig. 2) were collected from the upper part of the m1 section, which comprises calcite-rich marbles with quartzite intercalations (mm to several cm in thickness; generally less abundant and thinner than in the Panormos area). There is general consensus that these marbles belong to the BGU and thus were affected by HP metamorphism and a greenschist facies overprint.

The marbles are fine- to medium-grained, well-bedded rocks with white to bluish-grey colour on the outcrop- or hand-specimen scale. Individual layers rarely exceed 1 m in thickness. The total thickness of the marble sequences is highly variable, but may reach several tens of metres. In the Panormos area, m1 marbles often show a pebbly mudstone fabric with clasts and matrix consisting solely of carbonates. The clasts range in size from a few millimetres to several centimetres. Graded bedding and changes in grain size between individual layers were recognized locally. The mineral assemblage mostly consists of calcite; dolomite is present in some samples, but is always much less abundant. Among the accessories, phengite is most common, but albite, quartz, chlorite and graphite may occur in the groundmass as additional constituents. Phengite often is strongly enriched on bedding surfaces. Glaucophane, omphacite and/or garnet are not present.

ANALYTICAL METHODS

To characterize the white mica populations used for geochronological studies, phengite compositions were determined in six samples with the electron microprobe (EPM). For this purpose, polished thin-sections were prepared from white mica splits of the phengite separates used for ^{40}Ar–^{39}Ar and Rb–Sr dating, with the basal plane of mica plates positioned parallel to the surface of the glass slide. This orientation allowed systematic and representative EMP analysis of core and rim compositions. In addition, phengite compositions were determined in 'normal' polished thin-sections. For each sample *c.* 60–80 spots were analysed. With the exception of one sample, phengite compositions were determined with a SX-50 CAMECA microprobe at the Mineralogisches Institut, Universität Würzburg. Operating conditions were a 15 kV acceleration voltage, 10 nA beam current and counting time of 20–30 s. The beam diameter was set at 3–5 μm. Natural and synthetic mineral standards were used. The raw data were corrected with a ZAF procedure using the PAP software provided by Cameca. Phengite of sample 3016 was analysed with a JEOL JXA8600MX at the Institut für Mineralogie, Universität Münster. Operating conditions were a 15 kV acceleration voltage, 15 nA beam current and a counting time of 10 s. The beam diameter was set at 3–5 μm. Natural mineral standards were used. The raw data were corrected with a ZAF procedure. Representative phengite analyses are shown in Table 1.

Rb–Sr isotope analyses were carried out at the Zentrallaboratorium für Geochronologie at the Institut für Mineralogie, Universität Münster. For sample preparation, whole rocks (1–2 kg) were crushed in a steel mortar or using a jawbreaker and disc mill. For mica and calcite separation, crushed material was comminuted either by grinding for only a few seconds in a tungsten carbide mill or by use of a disc mill. Following sieving, fines were removed and mica was enriched by use of a Frantz magnetic separator and/or by adherence to a sheet of paper. After hand-picking, mica concentrates (optically pure $> 99\%$) were leached in acetic acid (4 M) for *c.* 30 s in an ultrasonic bath and afterwards repeatedly rinsed in ultrapure H_2O.

Phengite (*c.* 5–38 mg) and calcite (*c.* 44–65 mg) were mixed with a ^{87}Rb–^{84}Sr spike in Teflon screw-top vials and either dissolved in a HF–HNO_3 (5:1) mixture or in 2.5 N HCl on a hot plate overnight. After drying, 6 N HCl was added to the phengite residue. This mixture was homogenized on a hot plate overnight. After a second evaporation to dryness, Rb and Sr were separated by standard ion-exchange procedures (AG 50W-X8 resin) on quartz glass columns using 2.5 N HCl as eluent. Rb was loaded with H_2O on Ta filaments; Sr was loaded with TaF_5 on W filaments. Mass-spectrometric analysis was carried out using a VG Sector 54 multicollector mass spectrometer (Sr) and a NBS-type Teledyne mass spectrometer (Rb). Correction for mass fractionation is based on a $^{86}Sr/^{88}Sr$ ratio of 0.1194. Rb ratios were corrected for mass fractionation using a factor deduced from multiple measurements of Rb standard NBS 607. Total procedural blanks were less than 0.05 ng for Rb and 0.1 ng for Sr. Based on repeated measurements, the $^{87}Rb/^{86}Sr$ ratios were assigned an uncertainty of 1% (2σ). For the $^{87}Sr/^{86}Sr$ ratios, within-run uncertainties are reported at the $2\sigma_m$ level. In the course of this study, repeated runs of NBS standard 987 gave an average $^{87}Sr/^{86}Sr$ ratio of 0.710295 ± 0.000038 (2σ, $n = 15$), which is within the long-term average of the Münster

Table 1. Representative electron microprobe analyses of phengite from marbles, Tinos Island, Greece.

Marble	m3	m3	m3	m3	m2	m2	m2	m2	m1	m1	m1
Sample	3008A	3008A	3008A	3008A	3009B	3009B	3009B	3009B	3012B	3012B	3012B
Spot	4C	4R	11C	11R	7C	7R	16C	16R	1C	1R	4C
SiO_2	53.15	52.82	53.33	52.02	55.68	53.89	52.41	53.00	54.77	54.06	55.12
TiO_2	0.12	0.17	0.09	0.12	0.07	0.11	0.10	0.04	0.06	0.11	0.10
Al_2O_3	26.24	26.79	25.70	27.61	21.54	24.76	24.83	25.47	23.26	24.99	22.39
Cr_2O_3	0.00	0.00	0.05	0.04	0.00	0.08	0.07	0.16	0.16	0.05	0.04
MgO	4.88	4.77	4.91	4.41	6.43	5.59	5.13	5.14	6.20	5.54	6.42
CaO	0.00	0.04	0.00	0.04	0.00	0.02	0.01	0.00	0.04	0.00	0.05
MnO	0.00	0.00	0.04	0.00	0.01	0.00	0.00	0.00	0.00	0.00	0.02
FeO	0.31	0.29	0.30	0.26	1.16	0.99	1.18	0.93	0.07	0.15	0.20
BaO	0.02	0.04	0.02	0.10	0.29	0.50	0.49	0.44	0.05	0.03	0.09
Na_2O	0.19	0.22	0.11	0.36	0.08	0.12	0.20	0.18	0.07	0.11	0.06
K_2O	10.14	10.03	10.07	9.58	9.97	9.89	9.63	9.86	10.70	10.59	10.64
Total	95.05	95.16	94.60	94.54	95.22	95.95	94.05	95.20	95.38	95.64	95.12
Si	7.00	6.95	7.05	6.88	7.35	7.07	7.03	7.01	7.21	7.09	7.27
Ti	0.01	0.02	0.01	0.01	0.01	0.01	0.01	0.00	0.01	0.01	0.01
Al	4.07	4.15	4.00	4.30	3.35	3.83	3.92	3.97	3.61	3.86	3.48
Cr	0.00	0.00	0.00	0.00	0.00	0.01	0.01	0.02	0.02	0.01	0.00
Mg	0.96	0.94	0.97	0.87	1.27	1.09	1.02	1.01	1.22	1.08	1.26
Ca	0.00	0.01	0.00	0.01	0.00	0.00	0.00	0.00	0.01	0.00	0.01
Mn	0.00	0.00	0.00	0.00	0.00	0.00	0.00	0.00	0.00	0.00	0.00
Fe	0.03	0.03	0.03	0.03	0.13	0.11	0.13	0.10	0.01	0.02	0.02
Ba	0.00	0.00	0.00	0.01	0.01	0.03	0.03	0.02	0.00	0.00	0.00
Na	0.05	0.06	0.03	0.09	0.02	0.03	0.05	0.05	0.02	0.03	0.01
K	1.70	1.68	1.70	1.62	1.68	1.66	1.65	1.66	1.80	1.77	1.79
Total	13.83	13.83	13.80	13.81	13.82	13.84	13.85	13.85	13.88	13.87	13.88

Marble	m1	m1	m1	m1	m1	m1	m1	m1	m1	m1	m1
Sample	3012B	3013A	3013A	3013A	3013A	3013A	3013A	3014A	3014A	3014A	3014A
Spot	4R	6C	6R	10C	10R	19C	19R	12C	12R	15C	15R
SiO_2	55.37	54.31	54.14	54.36	54.21	54.35	53.81	55.39	55.56	54.61	52.86
TiO_2	0.12	0.08	0.07	0.04	0.08	0.07	0.13	0.12	0.12	0.17	0.41
Al_2O_3	22.64	23.69	23.33	23.06	23.28	23.79	24.35	21.16	21.24	22.43	23.71
Cr_2O_3	0.01	0.09	0.10	0.17	0.03	0.01	0.13	0.00	0.02	0.03	0.03
MgO	6.44	6.27	6.29	6.38	6.28	6.10	5.89	7.04	6.92	6.79	6.06
CaO	0.00	0.01	0.00	0.00	0.00	0.00	0.01	0.00	0.01	0.00	0.00
MnO	0.04	0.00	0.03	0.00	0.00	0.00	0.00	0.00	0.00	0.00	0.02
FeO	0.24	0.00	0.02	0.10	0.02	0.00	0.07	0.02	0.03	0.00	0.00
BaO	0.00	0.10	0.07	0.18	0.03	0.15	0.15	0.00	0.00	0.10	0.00
Na_2O	0.06	0.12	0.19	0.12	0.14	0.16	0.33	0.08	0.08	0.15	0.08
K_2O	10.51	10.71	10.62	10.73	10.39	10.74	10.46	10.71	10.94	10.74	10.92
Total	95.43	95.37	94.86	95.13	94.45	95.37	95.33	94.51	94.91	95.01	94.10
Si	7.27	7.15	7.17	7.19	7.19	7.16	7.09	7.35	7.35	7.22	7.07
Ti	0.01	0.01	0.01	0.00	0.01	0.01	0.01	0.01	0.01	0.02	0.04
Al	3.50	3.68	3.64	3.59	3.64	3.69	3.78	3.31	3.31	3.50	3.74
Cr	0.00	0.01	0.01	0.02	0.00	0.00	0.01	0.00	0.00	0.00	0.00
Mg	1.26	1.23	1.24	1.26	1.24	1.20	1.16	1.39	1.37	1.34	1.21
Ca	0.00	0.00	0.00	0.00	0.00	0.00	0.00	0.00	0.00	0.00	0.00
Mn	0.00	0.00	0.00	0.00	0.00	0.00	0.00	0.00	0.00	0.00	0.00
Fe	0.03	0.00	0.00	0.01	0.00	0.00	0.01	0.00	0.00	0.00	0.00
Ba	0.00	0.01	0.00	0.01	0.00	0.01	0.01	0.00	0.00	0.01	0.00
Na	0.01	0.03	0.05	0.03	0.04	0.04	0.08	0.02	0.02	0.04	0.02
K	1.76	1.80	1.79	1.81	1.76	1.80	1.76	1.81	1.85	1.81	1.86
Total	13.85	13.91	13.92	13.92	13.88	13.91	13.92	13.90	13.91	13.94	13.96

Number of cations based on 22 oxygen; C and R indicate core and rim, respectively.

laboratory. All ages and elemental concentrations were calculated using the IUGS recommended decay constants (Steiger & Jäger, 1977) by means of the Isoplot program version 2.49 (Ludwig, 1991). Rb–Sr isotope results are shown in Table 2.

Four samples were investigated with the $^{40}Ar/^{39}Ar$ technique at the Department of Geological Sciences, University of California, Santa Barbara. All $^{40}Ar/^{39}Ar$ dates were obtained by conventional step heating using a Staudacher-type resistance furnace. Flux monitors used were Taylor Creek Sanidine (US Geological Survey standard 85G003, Dalrymple & Duffield, 1988) with an assigned age of 27.92 Ma, and Charcoal Ovens Tuff, an internal standard with an assigned age of 35.88 Ma. Separates were packaged in copper and aluminium foil and loaded into a quartz vial with packaged flux monitors. Vials were irradiated at the TRIGA reactors at the USGS-Denver and Oregon State University for 30 h over a period of 5 days. Samples and monitors were heated in resistance furnace and gas was purified continuously during extraction by two SAES ST-172 porous getters and analysed on a MAP 216 mass spectrometer fitted with a Bauer-Signer source and a Johnston MM1 multiplier with a sensitivity of 2.0×10^{-14} mol V^{-1}. The resistance furnace uses a coiled tungsten filament, a tantalum crucible with no liner and tungsten–rhenium thermocouple. Analyses are blank-corrected and the typical system blanks on m/e 40 vary from 2.0×10^{-16} mol at low temperatures (< 1000 °C) and climb to 6.0×10^{-16} mol at 1300 °C for 15 min heating steps. All parts of the step-heating experiments are automated with pneumatically actuated, all-metal valves, a Macintosh computer and custom software.

Table 2. Rb–Sr isotope results for marbles from Tinos Island.

Sample	Unit	Mineral	Rb (ppm)	Sr (ppm)	$^{87}Rb/^{86}Sr$[a]	$^{87}Sr/^{86}Sr$	2σ	Age (Ma, 2σ)
3008	m3	Phengite[b]	285	0.89	976	1.277106	0.000056	41.1 ± 0.4
		Calcite[b]	0.11	153.6	0.00208	0.707326	0.000014	
3009	m2	Phengite[b]	226	76.85	8.52	0.711885	0.000036	37.2 ± 0.5
		Calcite[b]	0.07	407.6	0.000485	0.707390	0.000010	
3012	m1	Phengite[b]	276	3.24	248	0.792943	0.000026	24.2 ± 0.3
		Calcite[b]	0.27	291.4	0.00264	0.707659	0.000011	
3013	m1	Phengite[c]	173	10.89	46.2	0.723236	0.000049	23.9 ± 0.3
		Calcite[c]	0.12	268.7	0.00131	0.707572	0.000010	
3014	m1	Phengite[b]	190	2.53	218	0.783419	0.000088	24.5 ± 0.3
		Calcite[b]	0.03	464.0	0.000172	0.707628	0.000015	
3016	m3	Phengite[d]	367	9.83	109	0.761699	0.000013	34.9 ± 0.4
		Calcite[b]	0.03	145.3	0.000627	0.707627	0.000009	

[a]The $^{87}Rb/^{86}Sr$ ratios were assigned an uncertainty of 1% (2σ); [b] 355–250 μm; [c] 250–180 μm; [d] >355 μm.

RESULTS

Phengite compositions

All samples contain abundant high-Si phengite (Si > 3.45), that shows a rather restricted compositional variation (Figs 4 & 5; Table 1). With the exception of sample 3016, MgO concentrations range between 2.8 and 7.1 wt% and FeO concentrations are below 0.6 wt%. As a result, X_{Mg} values generally are >0.85 and mostly exceed 0.9. The three m1 samples show X_{Mg} values >0.95. The paragonite component [Na/(Na + K)] in phengite reaches up to 0.11. In samples 3009 and 3013 paragonite was recognized as a discrete phase. Besides homogeneous grains, chemical zoning is common, mostly indicating a decrease in celadonite content towards the rim (Table 1). It is important to record that rim compositions mostly still are Si-rich (Table 1).

Rb–Sr dating

Six samples from the three main marble sequences were selected for Rb–Sr geochronology using phengite–calcite pairs. Ages are reported in Table 2. Most studied phengite is characterized by low Sr concentrations (<1–11 ppm). Generally high Rb/Sr ratios (46–976) suggest that the ages are well constrained. The phengite separate of sample 3009 seems to be slightly contaminated by calcite, resulting in a higher Sr content (77 ppm) and a lower Rb/Sr ratio (8.5) than the other samples. Calcite has very low Rb concentrations (<0.5 ppm) and Sr contents in the range 147–480 ppm (Table 2). Similar values were obtained for phengite and calcite of m1 marbles from the Panormos area (M. Bröcker & L. Franz, unpubl. data).

Sample 3008, which represents the uppermost m3 marble between Isternia and Marlas, yielded an age of 41.1 ± 0.4 Ma. Sample 3016, collected from the m3 marbles near Mavra Gremna, provided a younger date of 35.1 ± 0.4 Ma (Table 2). At the roadcut between Isternia and Ormos Isternia, m2 marbles are exposed. Sample 3009 from this locality gave an age of 37.3 ± 0.5 Ma. The lowermost m1 marbles from Vathy (samples 3012, 3013, 3014; Table 2) yielded ages of 24.2 ± 0.3 Ma, 23.9 ± 0.3 Ma and 24.5 ± 0.3 Ma (weighted average: 24.2 ± 0.8 Ma). Rb–Sr data for m1 marbles from the Panormos area yielded ages between 22.9 and 25.1 Ma (weighted average: 24 ± 1 Ma, $n = 5$; M. Bröcker & L. Franz, unpubl. data).

Ar–Ar dating

Five phengite samples were analysed with the ^{40}Ar–^{39}Ar furnace step-heating method (Table 3). All gave disturbed age spectra. All samples showed similar gas release patterns and lower apparent ages in the low- and high-temperature steps, compared with higher apparent ages in the middle part of the spectra (Figs 5 & 6). Plateaus are not developed and the isotopic ratios do not yield linear arrays. High K/Ca ratios suggest that contamination with non-K-rich phases is not an issue. Two m3 marbles yielded total fusion ages of 42.7 ± 0.1 and 39.9 ± 0.1 Ma (Table 3; Fig. 6). Two m1 marbles gave ^{40}Ar–^{39}Ar ages of *c.* 27 Ma (Table 3; Fig. 7). With the exception of sample 3008, the total fusion ages systematically are 3–6 Ma higher than Rb–Sr ages from the same samples. In some spectra the young step ages from the low and high temperature steps correspond closely to the Rb–Sr age for the same samples (Figs 6 & 7).

DISCUSSION

Differences between Ar–Ar and Rb–Sr ages: general considerations

Marbles from three distinct lithostratigraphic levels of the BGU yielded white mica ages (^{40}Ar–^{39}Ar, Rb–Sr) that correspond closely to results previously reported from Tinos and other parts of the ACCB (e.g. Altherr *et al.*, 1979; Wijbrans & McDougall, 1986, 1988; Wijbrans *et al.*, 1990; Bröcker *et al.*, 1993; Bröcker & Franz, 1998). These studies have shown that ages around 53–40 Ma are related to blueschist facies metamorphism and that ages of *c.* 25–18 Ma indicate the timing of the greenschist facies overprint. Variable

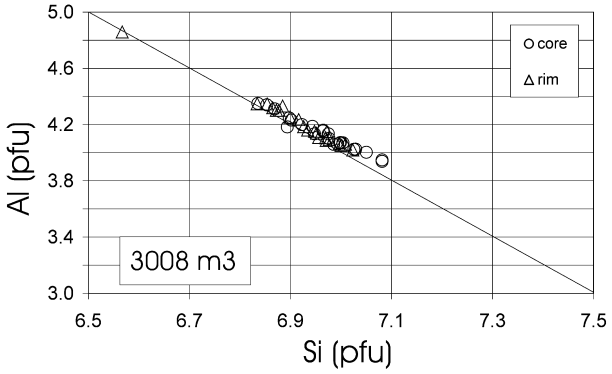

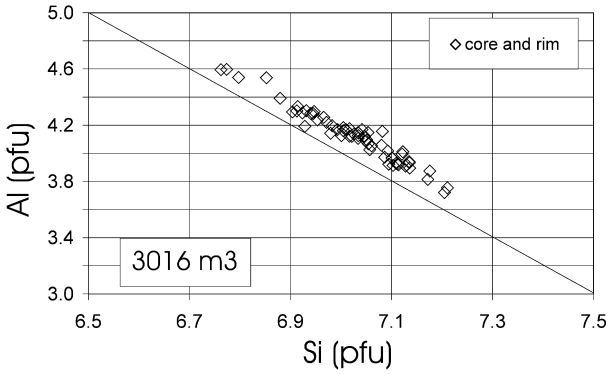

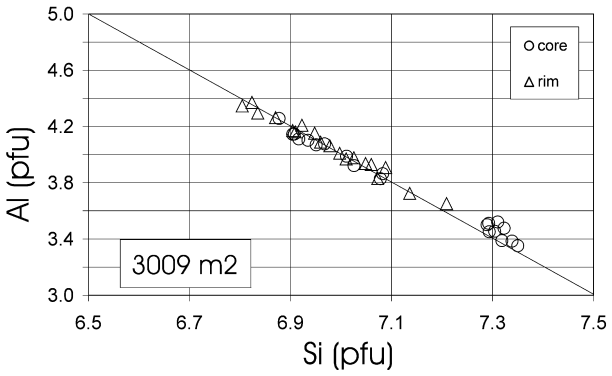

Fig. 4. Si-Al^{total} variation in phengite from m2 and m3 marbles.

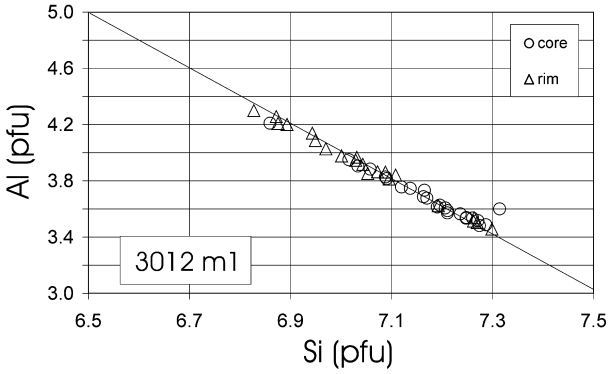

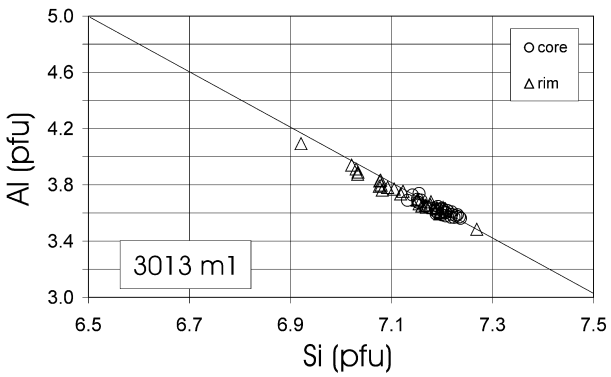

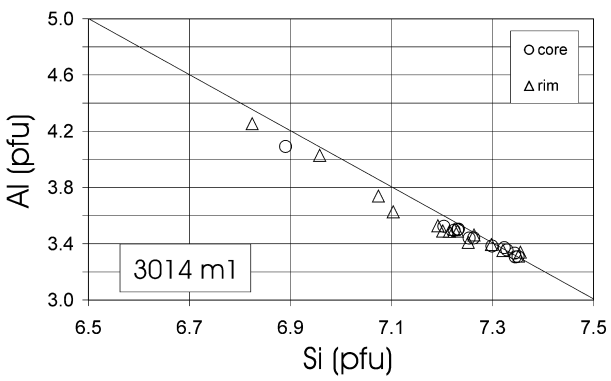

Fig. 5. Si-Al^{total} variation in phengite from m1 marbles.

degrees of retrogression and resetting are well documented by dates ranging between <40 and 25 Ma. Previous work on Tinos also showed that most of the Ar age spectra are disturbed and that ^{40}Ar–^{39}Ar ages of the HP rocks often are slightly older than Rb–Sr ages of the same samples (Bröcker *et al.*, 1993; Bröcker & Franz, 1998). For example, two well-preserved blueschists collected below the m3 marbles on Tinos yielded ^{40}Ar–^{39}Ar plateau ages of 43.8 ± 0.2 and 42.3 ± 0.2 Ma (Bröcker *et al.*, 1993); Rb–Sr ages from the same samples are 36.9 ± 0.4 and 39.0 ± 1.6 Ma (Bröcker & Franz, 1998).

The new results obtained on marbles (*c.* 41–24 Ma) fit perfectly into the previously established geochronological framework and complement existing data sets. All the Ar age spectra display disturbance and all ^{40}Ar–^{39}Ar total fusion ages are older than the Rb–Sr ages from the same samples (Figs 5 & 6; Tables 2 & 3). The total fusion dates of the m3 marbles (42.7 ± 0.1 and 39.9 ± 0.1 Ma) fall into the group of ages commonly recorded by HP rocks from the Cyclades and therefore can be interpreted as geologically meaningful. However, these dates provide no precise time constraints. The disturbed Ar release patterns (Figs 5 & 6; Table 3) suggest that the total fusion ages can only be considered to approximate the real age of the HP event. The two ^{40}Ar–^{39}Ar dates obtained on m1 marbles (*c.* 27 Ma; Fig. 7) exceed the age commonly recorded by greenschist facies samples from the study area (*c.* 25–18 Ma). The Rb–Sr date of the m3 marble

Table 3. Ar–Ar isotope results for phengite from marbles.

T	t	^{40}Ar (mol)	^{40}Ar/^{39}Ar	^{38}Ar/^{39}Ar	^{37}Ar/^{39}Ar	^{36}Ar/^{39}Ar	K/Ca	$\sum^{39}$Ar	^{40}Ar*	Age (Ma)
(a) Sample 3008 (J = 0.0042173)										
650	10	3.80E−14	8.239	0.00E+00	< 0	0.012	> 1000	0.0075	0.58	35.8 ± 0.4
750	10	1.40E−13	7.17	0.00E+00	0.0099	0.007	49	0.039	0.7	37.5 ± 0.1
790	10	2.80E−13	10.11	0.00E+00	0.0301	0.016	16	0.0835	0.54	41.1 ± 0.1
790	10	2.80E−13	7.029	0.00E+00	< 0	0.004	> 1000	0.1486	0.82	43.3 ± 0.1
770	10	1.20E−13	6.198	0.00E+00	< 0	0.001	> 1000	0.1811	0.93	43.4 ± 0.1
790	10	2.70E−13	6.471	0.00E+00	< 0	0.002	> 1000	0.249	0.9	43.8 ± 0.1
795	10	2.60E−13	6.384	0.00E+00	0.0025	0.002	198	0.3166	0.92	44 ± 0.1
795	10	2.30E−13	6.307	0.00E+00	< 0	0.002	> 1000	0.3771	0.93	44 ± 0.1
795	10	2.00E−13	6.288	0.00E+00	< 0	0.002	> 1000	0.4301	0.93	43.9 ± 0.1
800	10	1.90E−13	6.283	0.00E+00	< 0	0.002	> 1000	0.4798	0.93	43.8 ± 0.1
805	10	1.70E−13	6.253	0.00E+00	< 0	0.002	> 1000	0.5238	0.92	43.4 ± 0.1
810	10	1.50E−13	6.237	0.00E+00	< 0	0.002	> 1000	0.5638	0.92	43.2 ± 0.1
815	10	1.40E−13	6.215	0.00E+00	< 0	0.002	> 1000	0.5998	0.92	43.1 ± 0.1
820	10	1.20E−13	6.209	0.00E+00	< 0	0.002	> 1000	0.6319	0.92	42.9 ± 0.1
825	10	1.10E−13	6.211	0.00E+00	< 0	0.002	> 1000	0.6596	0.92	42.8 ± 0.1
830	10	8.90E−14	6.216	0.00E+00	< 0	0.002	> 1000	0.6829	0.91	42.6 ± 0.1
835	10	7.20E−14	6.242	0.00E+00	< 0	0.002	> 1000	0.7016	0.91	42.7 ± 0.1
840	10	5.80E−14	6.264	0.00E+00	< 0	0.002	> 1000	0.7167	0.9	42.5 ± 0.2
845	10	4.80E−14	6.299	0.00E+00	< 0	0.002	> 1000	0.7291	0.89	42.3 ± 0.2
850	10	4.10E−14	6.343	0.00E+00	< 0	0.002	> 1000	0.7397	0.89	42.4 ± 0.2
855	10	3.70E−14	6.386	0.00E+00	< 0	0.003	> 1000	0.7493	0.88	42.4 ± 0.3
875	10	5.10E−14	6.434	0.00E+00	< 0	0.003	> 1000	0.7623	0.88	42.4 ± 0.2
900	10	8.90E−14	6.532	0.00E+00	< 0	0.003	> 1000	0.7845	0.88	43 ± 0.1
925	10	1.80E−13	6.438	0.00E+00	< 0	0.002	> 1000	0.8293	0.89	43 ± 0.1
950	10	2.80E−13	6.139	0.00E+00	0.0114	0.002	43	0.9032	0.91	42.2 ± 0.1
950	10	9.60E−14	5.845	0.00E+00	< 0	0.002	> 1000	0.93	0.92	40.4 ± 0.1
950	10	4.40E−14	5.772	0.00E+00	< 0	0.002	> 1000	0.9426	0.92	39.8 ± 0.2
955	10	3.00E−14	5.75	0.00E+00	< 0	0.002	> 1000	0.951	0.92	39.8 ± 0.3
975	10	3.20E−14	5.781	0.00E+00	< 0	0.002	> 1000	0.9599	0.92	39.9 ± 0.3
1000	10	2.90E−14	5.786	0.00E+00	< 0	0.001	> 1000	0.9682	0.93	40.3 ± 0.3
1030	10	2.50E−14	5.795	0.00E+00	< 0	0.001	> 1000	0.9753	0.94	40.8 ± 0.3
1070	10	3.80E−14	6.141	0.00E+00	< 0	0.001	> 1000	0.9855	0.93	43.1 ± 0.2
1120	10	5.40E−14	6.091	0.00E+00	< 0	0.001	> 1000	1	0.93	42.8 ± 0.2
Total fusion age, TFA = 42.71 ± 0.07 Ma (including J).										
Weighted mean plateau age, WMPA = 42.80 ± 0.07 Ma (including J).										
Inverse isochron age = 44.00 ± 0.28 Ma. (MSWD = 1.99; ^{40}Ar/^{36}Ar = 207.1 ± 19.7).										
Steps used: 815, 820, 825, 830, 835, 840, 845, 850, 855, 875, (13–22/33 or 20% Σ^{39}Ar).										
(b) Sample 3013 (J = 0.0042157)										
650	10	8.80E−15	6.914	0.00E+00	0.3804	0.014	1.3	0.008	0.42	21.7 ± 1.2
730	10	2.10E−14	5.261	0.00E+00	0.0209	0.007	23	0.0325	0.6	23.9 ± 0.4
770	10	2.20E−14	4.682	0.00E+00	0.0115	0.005	42	0.0615	0.69	24.5 ± 0.3
790	10	2.30E−14	5.432	0.00E+00	0.0109	0.007	45	0.0887	0.6	24.7 ± 0.3
800	10	2.90E−14	6.658	0.00E+00	< 0	0.011	> 1000	0.1159	0.52	25.9 ± 0.4
810	10	3.70E−14	5.776	0.00E+00	0.0008	0.008	646	0.1556	0.61	26.8 ± 0.2
820	10	4.20E−14	4.903	0.00E+00	< 0	0.004	> 1000	0.2088	0.73	27.1 ± 0.2
830	10	4.60E−14	4.634	0.00E+00	< 0	0.003	> 1000	0.2705	0.79	27.5 ± 0.2
850	10	7.50E−14	4.549	0.00E+00	0.0047	0.003	104	0.3735	0.82	28.0 ± 0.1
880	10	1.30E−13	4.52	0.00E+00	< 0	0.003	> 1000	0.5542	0.83	28.2 ± 0.1
900	10	8.30E−14	4.44	0.00E+00	< 0	0.003	> 1000	0.6715	0.82	27.3 ± 0.1
920	10	4.70E−14	4.451	0.00E+00	< 0	0.003	> 1000	0.7383	0.79	26.6 ± 0.2
940	10	3.20E−14	4.398	0.00E+00	< 0	0.003	> 1000	0.7844	0.81	26.9 ± 0.2
980	10	3.40E−14	4.146	0.00E+00	0.0028	0.003	175	0.8359	0.83	25.8 ± 0.2
1030	10	1.90E−14	4.583	0.00E+00	< 0	0.004	> 1000	0.8613	0.75	26.0 ± 0.4
1090	10	4.70E−14	4.366	0.00E+00	0.0075	0.003	65	0.929	0.82	26.9 ± 0.1
1150	10	5.00E−14	4.426	0.00E+00	0.0035	0.003	138	1	0.81	26.9 ± 0.1
Total fusion age, TFA = 26.97 ± 0.06 Ma (including J).										
Weighted mean plateau age, WMPA = 26.87 ± 0.08 Ma (including J).										
Inverse isochron age = 26.83 ± 0.20 Ma. (MSWD = 1.15; ^{40}Ar/^{36}Ar = 296.8 ± 7.1).										
Steps used: 810, 820, 920, 940, 1090, 1150, (6–17/17 or 34% Σ^{39}Ar).										
(c) Sample: 3014 (J = 0.0042129)										
650	10	1.40E−14	5.574	6.70E−03	0.236	0.008	2.1	0.0047	0.57	24.0 ± 0.7
730	10	3.30E−14	4.381	3.00E−04	0.0733	0.004	6.7	0.0187	0.76	25.2 ± 0.2
770	10	7.10E−14	7.113	0.00E+00	< 0	0.013	> 1000	0.0375	0.48	25.5 ± 0.2
790	10	1.10E−13	6.828	0.00E+00	< 0	0.011	> 1000	0.0685	0.52	27.0 ± 0.1
800	10	1.10E−13	4.664	0.00E+00	0.0011	0.004	451	0.1132	0.78	27.4 ± 0.1
810	10	1.20E−13	4.288	0.00E+00	0.0001	0.002	6951	0.1651	0.85	27.4 ± 0.1
820	10	1.60E−13	4.221	0.00E+00	0	0.002	> 1000	0.2351	0.87	27.6 ± 0.1
830	10	2.20E−13	4.205	0.00E+00	0.0012	0.002	396	0.334	0.88	27.9 ± 0.1
850	10	3.30E−13	4.149	0.00E+00	0.0035	0.002	141	0.4844	0.89	27.9 ± 0.0
850	10	2.10E−13	4.031	0.00E+00	< 0	0.001	> 1000	0.583	0.9	27.2 ± 0.1
880	10	2.50E−13	3.886	0.00E+00	0.0014	0.001	356	0.7021	0.9	26.4 ± 0.0
900	10	1.50E−13	3.807	0.00E+00	< 0	0.001	> 1000	0.7768	0.89	25.7 ± 0.1
920	10	1.20E−13	3.905	0.00E+00	0.0025	0.002	193	0.8345	0.89	26.2 ± 0.1

Table 3. (*Cont'd.*)

T	*t*	^{40}Ar (mol)	^{40}Ar/^{39}Ar	^{38}Ar/^{39}Ar	^{37}Ar/^{39}Ar	^{36}Ar/^{39}Ar	K/Ca	$\sum^{39}$Ar	^{40}Ar*	Age (Ma)
940	10	1.20E−13	3.944	0.00E + 00	0.001	0.001	472	0.8894	0.9	26.6 ± 0.1
960	10	8.60E−14	3.832	0.00E + 00	< 0	0.001	> 1000	0.9311	0.91	26.2 ± 0.1
990	10	3.90E−14	3.677	0.00E + 00	< 0	0.001	> 1000	0.9508	0.91	25.3 ± 0.1
1030	10	1.70E−14	3.64	0.00E + 00	< 0	0.001	> 1000	0.9596	0.9	24.6 ± 0.3
1080	10	1.20E−14	3.765	0.00E + 00	0.0171	0.001	29	0.9657	0.9	25.5 ± 0.5
1150	10	7.10E−14	3.888	0.00E + 00	0.0083	0.001	59	1	0.91	26.7 ± 0.1
Total fusion age, TFA = 26.92 ± 0.04 Ma (including J).										
Weighted mean plateau age, WMPA = 27.26 ± 0.04 Ma (including J).										
Inverse isochron age = 26.96 ± 0.30 Ma. (MSWD = 126.58; ^{40}Ar/^{36}Ar = 300.1 ± 15.7).										
Steps used: (1–19/19 or 100% Σ^{39}Ar).										
(d) Sample: 3016 (J = 0.0042112)										
650	10	1.90E−14	8.764	8.50E−03	25.2123	0.015	0.019	0.0077	0.49	32.1 ± 3.3
730	10	4.20E−14	6.685	8.20E−04	14.1452	0.007	0.035	0.0299	0.69	34.5 ± 1.6
770	10	6.90E−14	8.402	0.00E + 00	0.0382	0.012	13	0.0588	0.57	35.7 ± 0.2
790	10	2.00E−13	8.021	0.00E + 00	0.0127	0.009	39	0.1452	0.68	40.9 ± 0.1
800	10	2.40E−13	6.158	0.00E + 00	0.0053	0.002	93	0.2801	0.89	41.1 ± 0.1
810	10	2.50E−13	5.948	0.00E + 00	0.0029	0.002	171	0.4278	0.92	41.2 ± 0.1
820	10	2.10E−13	5.873	0.00E + 00	0.0014	0.001	346	0.5508	0.93	41.0 ± 0.1
830	10	1.40E−13	5.812	0.00E + 00	0.0039	0.001	127	0.6349	0.93	40.5 ± 0.1
850	10	1.20E−13	5.77	0.00E + 00	0.0026	0.002	189	0.7067	0.92	39.8 ± 0.1
880	10	1.10E−13	5.851	0.00E + 00	< 0	0.002	> 1000	0.7705	0.91	39.8 ± 0.1
900	10	8.00E−14	5.927	0.00E + 00	0.0102	0.002	48	0.8179	0.89	39.7 ± 0.1
920	10	7.90E−14	5.717	0.00E + 00	0.0045	0.002	108	0.8667	0.91	38.9 ± 0.1
940	10	6.90E−14	5.531	0.00E + 00	0.0058	0.002	85	0.9103	0.91	38.0 ± 0.1
960	10	3.20E−14	5.263	0.00E + 00	0.0213	0.002	23	0.9317	0.92	36.2 ± 0.3
990	10	1.70E−14	5.122	0.00E + 00	0.0291	0.002	17	0.9434	0.89	34.4 ± 0.5
1030	10	2.10E−14	5.331	0.00E + 00	0.011	0.002	44	0.9574	0.91	36.3 ± 0.4
1080	10	5.10E−14	5.729	0.00E + 00	0.0127	0.002	39	0.9889	0.92	39.7 ± 0.2
1150	10	1.80E−14	5.791	0.00E + 00	0.0667	0.002	7.3	1	0.9	39.1 ± 0.5
Total fusion age, TFA = 39.86 ± 0.08 Ma (including J).										
Weighted mean plateau age, WMPA = 41.08 ± 0.07 Ma (including J).										
Inverse isochron age = 41.14 ± 0.11 Ma. (MSWD = 3.48; ^{40}Ar/^{36}Ar = 291.9 ± 3.9).										
Steps used: 790, 800, 810, 820, (4–7/18 or 49% Σ^{39}Ar).										

t = dwell time in minutes. ^{40}Ar(mol) = moles corrected for blank and reactor-produced ^{40}Ar. Ratios are corrected for blanks, decay, and interference. $\sum^{39}$Ar is cumulative, ^{40}Ar* = rad fraction.

3008 indicates a 'typical' HP age (41.1 ± 0.4 Ma), whereas the considerably younger date provided by m3 sample 3016 (35.1 ± 0.4 Ma) suggests partial resetting during the overprint. M1 marbles dated in this and previous studies yielded Rb–Sr ages of *c*. 24 Ma (Fig. 7; Table 2; M. Bröcker & L. Franz, unpubl. data), and thus are within the age range commonly found for greenschist facies rocks in the ACCB.

It is still unclear which processes may have caused the complexities in the ^{40}Ar–^{39} spectra and the higher apparent Ar ages compared with the Rb–Sr method. Two contrasting interpretations previously were suggested to explain the age difference, emphasizing either variable disturbance of the Rb–Sr isotope system during overprinting (Bröcker & Franz, 1998), or contamination by excess Ar (Altherr *et al.*, 1979; Sherlock & Kelley, 2002). Complex ^{40}Ar–^{39}Ar spectra of Cycladic rocks were also related to heterogeneous resetting, due to localized recrystallization caused by strongly partitioned deformation (Baldwin & Lister, 1998). Modelling by these authors suggests that Oligocene–Miocene overprinting was of insufficient magnitude and/or duration to completely reset the Ar isotope system.

To shed more light on this puzzling record and to obtain a wider understanding of the mechanism controlling the shape of the Ar age spectra, the following potential explanations should be taken into consideration: (a) the white mica populations represent mixtures of different phengite generations with distinct ages; (b) the white mica populations consist of phengite and paragonite, which show different degassing behaviour; (c) the complex spectra are caused by the incorporation of excess Ar (^{40}Ar not related to *in situ* radioactive decay of ^{40}K), that was added during or after phengite formed; (d) the phengite was unable to lose ^{40}Ar during the overprint and therefore is variably contaminated by an inherited component. These options provide explanations for the disturbed Ar age spectra and may also account for the difference between the apparent ^{40}Ar–^{39}Ar and Rb–Sr ages. However, a fifth option (e) is that the overprint affected the Rb–Sr system to a larger extent than the K–Ar system. In our view, a combination of alternatives (d) and (e) best explains the disturbed Ar spectra and the trend towards younger Rb–Sr dates for the following reasons. The white mica populations consist mostly of high-Si phengite. Based on textural observations and white mica chemistry different phengite generations cannot be distinguished. Paragonite was only recognized in two samples (3009, 3013) in relatively small amounts and therefore is unlikely to have significantly influenced the general picture. Within-grain zonation was recognized in some phengite – decreasing celadonite contents from core to

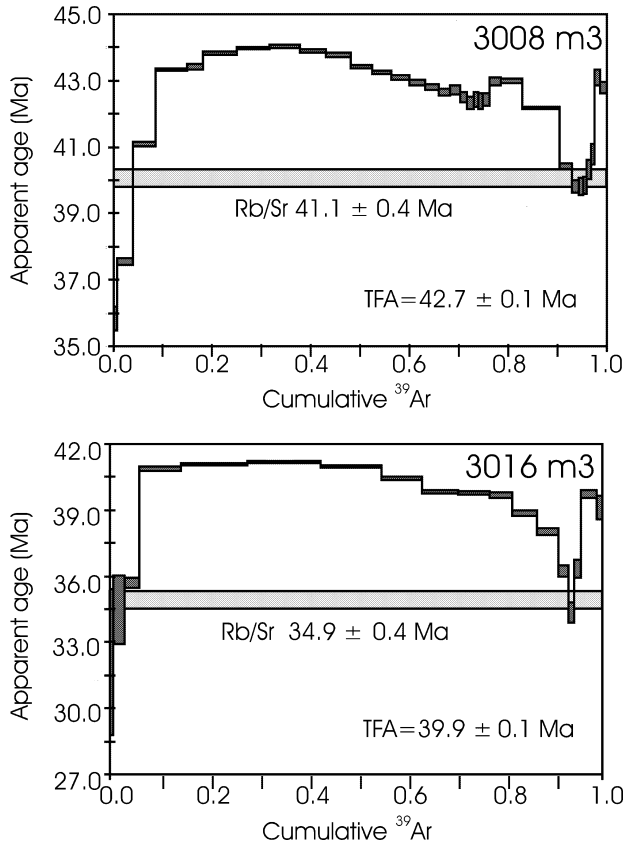

Fig. 6. ^{40}Ar–^{39}Ar age spectra for phengite from m3 marbles (TFA = total fusion age). The corresponding Rb–Sr age (phengite–calcite) is indicated by a horizontal bar.

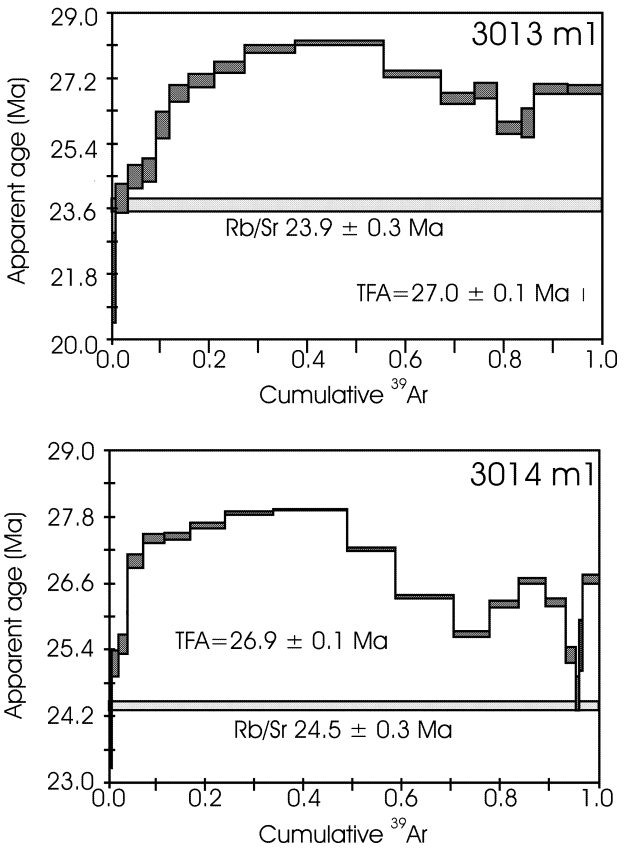

Fig. 7. ^{40}Ar–^{39}Ar age spectra for phengite from m1 marbles (TFA = total fusion age). The corresponding Rb–Sr age (phengite–calcite) is indicated by a horizontal bar.

rim – but the rim composition still has high Si contents (Table 1). This zonation possibly indicates variations in metamorphic conditions during the HP stage. However, as will be discussed below, a relationship to the greenschist facies overprint seems to be a reasonable alternative, due to bulk-compositional controls on the Tschermaks substitution. Thus, mixing of phengite, which represents geochronologically distinct stages of the *P–T* path remains an option to explain the disturbed spectra, but is not our favoured interpretation, because it provides no convincing explanation for the age difference between both dating techniques. More reasonable is the assumption that contamination with extraneous argon (either excess or inherited ^{40}Ar) is of major importance. The presence of excess ^{40}Ar leading to geologically meaningless dates was documented for many HP and UHP occurrences (e.g. Li *et al.*, 1994; Arnaud & Kelley, 1995; Hacker & Wang, 1995; Scaillet, 1998 and references therein; El-Shazly *et al.*, 2001). In such cases, the Ar age spectra of contaminated samples may show plateaus with ages significantly older than those provided by other isotopic systems and which are in conflict with the general geological background of the study area. To interpret the rocks discussed here, it is important to note that neither the total fusion ages nor the step ages are older than the timing of the HP event, as constrained by concordant K–Ar and Rb–Sr phengite ages on Sifnos (*c.* 42 Ma, Altherr *et al.*, 1979), or by concordant ages from Syros (*c.* 53 Ma) that are based on ^{40}Ar–^{39}Ar paragonite and SHRIMP U–Pb zircon dating (Tomaschek *et al.*, 2003). Furthermore, the total fusion ages of the studied samples are not very different to the corresponding Rb–Sr ages. This indicates that contamination with extraneous Ar was limited. Due to the polymetamorphic history, we consider inheritance from the HP stage as the most likely cause for the complex ^{40}Ar–^{39}Ar age spectra and the trend towards older Ar dates.

It is possible that the younger Rb–Sr ages still do not indicate the true age of overprinting. However, the fact that these ages are within the range commonly observed for greenschist facies rocks in the ACCB suggests that these ages are geologically relevant. In the present case, there is no doubt that the Rb–Sr system reacted more sensitively to the overprinting than the Ar isotope system. The difference between apparent ^{40}Ar–^{39}Ar and Rb–Sr ages of the marbles may be explained by the fact that resetting of the Sr isotope system during the greenschist overprint can easily be accomplished by Sr exchange with the surrounding

calcite. In contrast, only sluggish and limited rejuvenation, resulting in partial inheritance, can be expected for the Ar isotope system in carbonate rocks, especially in the absence of pervasive deformation and/or if availability of synmetamorphic fluids is restricted. The model suggesting faster resetting of the Rb–Sr system due to much easier Sr than Ar exchange most likely also holds true for the resetting of white mica in other bulk compositions with mineral assemblages that comprise abundant Ca-rich phases (e.g. epidote, Ca-amphibole, calcite). As already pointed out by Giorgis *et al.* (2000), it can be expected that in this case the Sr isotope system responds more rapidly during retrogression than the Ar isotope system, because Sr can more easily be partitioned into coexisting phases.

Miocene HP metamorphism in the m1 marbles on Tinos?

Under favourable circumstances, the record of earlier stages in the pre-metamorphic or tectonomorphic evolution can be documented by Rb–Sr and ^{40}Ar–^{39}Ar geochronology of mica, despite severe overprinting. For example, Kühn *et al.* (2000) reported from the Bergen Arc Complex (Norway) the retention of Rb–Sr phlogopite ages, which were related to Precambrian granulite facies metamorphism, through Caledonian HP metamorphism at minimum temperatures of at least 650 °C. Maurel *et al.* (2003) described pre-metamorphic ^{40}Ar–^{39}Ar biotite ages from the French Variscan belt, which survived overprints under HP and amphibolite facies conditions at temperatures more than 400 °C above those normally estimated for Ar retention in biotite. The preservation of Eocene ages in relic HP rocks of the Cyclades (e.g. Bröcker *et al.*, 1993) is one of the many examples where the geochronological record of an earlier metamorphic episode survived overprinting at temperatures close to the closure temperature. Retention of the argon isotope system in mica is directly coupled to the mobility of the structure-forming major elements (e.g. Di Vincenzo *et al.*, 2001), and a similar behaviour can reasonably be assumed for the Rb–Sr system. This implies that the geochronological record of an earlier metamorphic episode can survive a subsequent overprint if the relict chemistry of the dated mica is preserved. Lack of fluid infiltration and/or the absence of pervasive deformation are considered to be the main factors controlling the resistance of the original isotopic signature (e.g. Bröcker *et al.*, 1993; Kühn *et al.*, 2000; Maurel *et al.*, 2003).

The upper part of the m1 sequence – from which we collected the samples discussed here – is generally considered to be an integral part of the BGU (Melidonis, 1980; Avigad & Garfunkel, 1989; Bröcker, 1990a), which has a well-documented record of eclogite- to blueschist facies metamorphism and greenschist facies overprinting (e.g. Bröcker *et al.*, 1993). The blueschist-to-greenschist transition was essentially catalysed by the availability of a synmetamorphic fluid (Bröcker, 1990a,b). In non-infiltrated rock volumes, the HP assemblages persisted, whereas fluid influx caused retrogression. In the middle and upper parts of the BGU, domains of relic HP rocks are preserved in more-overprinted rock volumes; in some places HP rocks and their greenschist facies counterparts occur in interlayered sequences. Field observations indicate channelled infiltration of a fluid phase, presumably controlled by differences of permeability and/or structural factors (Bröcker, 1990a,b; Bröcker *et al.*, 1993). Even in strongly overprinted samples, relics of the HP stage (glaucophane, garnet, high-Si phengite) often are recognized. Due to these field and textural observations, it would not come as a surprise to find also some HP rocks at lower lithostratigraphic levels of the BGU, although previous work indicated that this part is more strongly affected by the overprint (Bröcker & Franz, 1998; Matthews *et al.*, 1999). Thus, at first sight, the high-Si phengite of the m1 marbles appears to be related to HP metamorphism. This working hypothesis is apparently further supported by findings of glaucophane-bearing relics of HP rocks directly above the m1 marbles in the Panormos area. On the basis of the general geological background, it appears reasonable to expect for the m1 marbles ages that are similar to those commonly reported for HP rocks in the Cyclades. Nevertheless, the high-Si phengite of the m1 marbles yielded typical greenschist facies ages. Pressure and age results obtained from the same phengite appear to be decoupled. This apparent paradox is addressed next.

The silica content in phengite is pressure dependent in silicate rocks (Velde, 1967; Massonne & Schreyer, 1987; Massonne, 1991), due to the $Al^{IV} + Al^{VI} = Si^{IV} + (Mg + Fe)^{VI}$ Tschermaks or celadonite substitution. As a consequence, the Si content in phengite coexisting with a limiting mineral assemblage (e.g. K-feldspar, biotite, quartz, H_2O) constrains the metamorphic pressure for a given temperature in granitic bulk compositions; a minimum pressure can be deduced if phengite does not occur in the limiting assemblage (Massonne & Schreyer, 1987; Massonne, 1991).

Caution is warranted in interpreting phengite compositions alone as an indicator for metamorphic pressures. The presence of high-Si phengite (Si > 3.5 p.f.u.) in a rock that lacks typical HP assemblages or index minerals (e.g. glaucophane, omphacite) does not provide unequivocal evidence for an earlier blueschist- or eclogite facies episode. For example, depending on bulk composition (e.g. low Al_2O_3), high-Si phengite can also occur in silicate-rich rocks not affected by HP metamorphism (Guidotti & Sassi, 1976, 1986; Sassi *et al.*, 1994). The m1 marbles carry no typical HP mineral assemblage and subordinate silicate phases only comprise phengite, albite, chlorite and quartz. This mineral assemblage is not indicative of HP conditions, although the phengite generally is Si-rich.

What is the explanation for the apparent discrepancy between the petrological and the geochronological

record? In our view, the high-Si phengite in the m1 marbles does not represent relics of the HP stage. As indicated by the young ages, the m1 marbles must have been affected by pervasive retrogression under greenschist facies P–T conditions, which caused a partial to complete resetting of the Ar and Rb–Sr isotope systems in phengite. The structure-forming major elements in phengite largely remained unaffected by resetting during the overprint – major element abundances did not change during recrystallization – due to bulk-compositional controls. Two alternatives must be considered: (1) The Si budget of the whole rock system is rather restricted. Only small amounts of silicates occur in the calcite marbles. Among these, white mica is the most common or the only silicate phase and therefore available Si is mostly be partitioned into phengite. (2) The m1 marbles typically are intercalated with quartzites. Si from this reservoir is redistributed by synmetamorphic fluids and mostly is accommodated by phengite, which is the major sink for Si in these mineralogically confined rocks.

Whatever interpretation is considered to be more likely, the fact remains that the Si-in-phengite values are mainly a function of bulk chemistry and/or fluid composition, due to the lack of a buffering assemblage. Under closed system conditions, significant modifications of an original HP phengite by retrograde chemical exchange is unlikely. Exchange reactions can only be expected by interaction with externally derived fluids, but also in this case are strongly controlled by the composition of synmetamorphic fluids, which may or may not allow changes in phengite chemistry. The fact that the HP ages were not retained indicates that the phengite underwent (fluid-enhanced) recrystallization. It is unlikely that the radiogenic isotope systems were reset but that the major elements were not. Due to bulk-compositional controls, the high-Si contents of the marbles are unrelated to metamorphic pressures. This interpretation explains the observation that high-Si phengite from different marbles within a structurally coherent succession yielded significantly different metamorphic ages (Table 1). These marbles were affected by variable degrees of greenschist facies overprinting.

Phengite chemistry cannot distinguish between samples providing HP ages, partially reset ages or ages related to the greenschist facies overprint. The Si-in-phengite criterion alone is only of limited use for correct identification of the metamorphic event that is dated by white mica geochronology. If the polymetamorphic evolution is not taken into consideration or unknown, and if phengite barometry is uncritically applied, the combination of high-Si contents with ages of *c*. 24 Ma may lead to the erroneous conclusion that the m1 marbles have experienced HP metamorphism at the Oligocene–Miocene boundary. The fact is that the Rb–Sr phengite ages of the m1 marbles document the timing of the overprint and do not testify to a Oligocene/Miocene blueschist event that has so far gone unnoticed in the central Cyclades. The ^{40}Ar–^{39}Ar dates are slightly older due to partial inheritance from the HP stage.

In other lithologies from the study area (e.g. clastic metasediments, metabasic and meta-acidic rocks), the range in Si contents and the modal proportion of phengite with a specific Si value are not significantly different between HP rocks and greenschist facies samples (Bröcker *et al*., 1993; Bröcker & Franz, 1998). Besides incomplete resetting during overprinting, this feature is related to the fact that Si-in-phengite only records the minimum pressures attained during metamorphism, if phengite does not occur in the limiting assemblage (Massonne & Schreyer, 1987). As already observed for the marbles, phengite chemistry alone provides no unambiguous information about the metamorphic stage that is dated by white mica geochronology. Only when based on P–T sensitive mineral assemblages can mica ages be correctly assigned to distinct metamorphic episodes.

Regional implications

The Cretan detachment is a north-dipping, low-angle normal fault in the Aegean Sea that developed subparallel to a subjacent subduction thrust in the early Miocene (Jolivet *et al*., 1996; Thomson *et al*., 1998; Ring & Reischmann, 2002). Petrological and chronological results reported from basal units underlying the CBU on the islands of Samos, Evvia and Tinos provided key arguments for suggesting large displacement (>100 km) and extreme slip rates (>20 km Ma^{-1}) along this detachment (Ring *et al*., 2001; Ring & Reischmann, 2002). The basal units are considered to represent para-authochthonous units that are separated from the structurally higher Cycladic blueschist sequences by thrust faults. The presence of high-Si phengite in such sequences, dated at *c*. 24–20 Ma, was taken as evidence that the basal units were in close proximity to the Plattenkalk–Phyllite–Quartzite unit (Crete) during the Miocene, and together were affected by contemporaneous HP metamorphism (Ring *et al*., 2001). These authors concluded that the rocks on Crete and in the Cyclades were subsequently displaced more than 100 km along the Cretan detachment, thereby suggesting one of the greatest displacements ever recognized for a detachment fault.

Our study on Tinos is not related to the basal units and thus does not complement the existing database used for the above-mentioned tectonic models. However, the results of our work in a structurally higher tectonic unit of the ACCB bear general implications for the interpretation of white mica ages from polymetamorphic terranes. We are concerned that a basic prerequisite for the aforementioned geodynamic model and the underlying idea of Miocene HP metamorphism may be unfounded. To treat this problem in detail, we re-evaluate the geochronological database used to

support the concept of mega-detachments, focusing on the interpretation of phengite ages. A general discussion of the palinspastic reconstruction of Ring *et al.* (2001) is beyond the scope of this paper.

Tectonic windows that expose the rock sequences beneath the Cycladic blueschist–greenschist sequences were reported from Tinos, Evvia and Samos (Avigad & Garfunkel, 1989; Shaked *et al.*, 2000; Ring *et al.*, 2001). Based on the presence of Si-rich phengite and/or glaucophane relics in rocks mainly comprising greenschist facies or mineral assemblages that are not facies specific, HP metamorphism was suggested for these occurrences, but the potential influence of the subsequent overprint on the isotope systems was ignored. Phengite ages (^{40}Ar–^{39}Ar and/or Rb–Sr) obtained on such samples from three widely separated islands are *c.* 23 Ma (Bröcker & Franz, 1998; Ring *et al.*, 2001; Ring & Reischmann, 2002), leading to the conclusion that the basal units experienced HP metamorphism at this time.

On Samos, the Kerketas nappe (=basal unit) mostly consists of dolomitic marbles (>1500 m), with minor intercalations of metapelites and impure marbles, that experienced HP metamorphism followed by a greenschist facies overprint (Ring *et al.*, 2001). Metapelites carry typical greenschist facies assemblages without relics of glaucophane. Impure marbles mainly consist of calcite, quartz, phengite and chlorite. Rare talc was recognized. The impure marbles selected for geochronology contain Si-rich phengite belonging solely to the 3T polytype (Ring *et al.*, 2001). This polymorph is considered to indicate formation under HP conditions (e.g. Sassi *et al.*, 1994); the presence of phengite–talc assemblages is compatible with this conclusion (Massonne & Schreyer, 1989). Ring *et al.* (2001) mostly obtained ^{40}Ar–^{39}Ar and Rb–Sr ages between 24 and 21 Ma. One sample with a ^{40}Ar–^{39}Ar date of 27.1 ± 1.0 Ma (isochron age: 25.2 ± 3.2 Ma) was interpreted to be contaminated with excess Ar. The only sample that was dated with both the ^{40}Ar–^{39}Ar and Rb–Sr methods provided a younger Rb–Sr age (23.7 ± 0.4 and 20.8 ± 0.2 Ma, respectively). The phengite ages of the impure marbles (24–21 Ma) were interpreted to date the HP event. At first sight, this seems a reasonable conclusion because the 3T polytype is believed to easily invert to the $2M_1$ polytype during retrogression. However, the general relationships between mica polytypism and isotope systematics are ambiguous. For example, Altherr *et al.* (1979) reported that samples from Sifnos show a clear correlation between mica polytypism, metamorphic grade and white mica ages (K–Ar, Rb–Sr). Mica populations of well-preserved HP rocks that mainly consist of 3T phengite yielded ages of *c.* 42 Ma, whereas $2M_1$ phengite from greenschist facies rocks provided ages of 24–21 Ma. In contrast, Wijbrans *et al.* (1990) described from the same island coexisting 3T and $2M_1$ phengite in HP rocks and overprinted greenschist facies samples, single grain argon laser probe ages of *c.* 42 and 30 Ma for both groups, and no significant age difference between different polytypes from the same samples. In the context discussed here, the fact that 3T phengite yielded reset ages (*c.* 30 Ma) is of special importance. An obvious relationship between mica polytype, metamorphic grade and age is not realized. Furthermore, Ring *et al.* (2001) emphasized that the dated phengite was not affected by greenschist facies recrystallization, because EMP mapping indicated no chemical zoning. However, the phengite population shows a range in Si-values (3.3–3.5), which might be related to recrystallization. We also note that similar ranges were reported for both HP and overprinted, age-reset rocks in the overlying CBU (e.g. Bröcker *et al.*, 1993). Thus, the conclusions of Ring *et al.* (2001) cannot unambiguously be demonstrated. Taking all this into account, we doubt that the age of the HP event is Miocene.

Also questionable is the interpretation of the ages from Tinos and Evvia. The status of the basal sequence on Tinos as a distinct tectonic subunit is controversial. Bröcker & Franz (submitted) recently interpreted the 'basal unit' as an integral part of the CBU, as originally suggested by Melidonis (1980). Furthermore, the age from Tinos, cited by Ring & Reischmann (2002) as evidence for Miocene HP metamorphism, refers to a calcschist with a greenschist facies mineral assemblage (Bröcker & Franz, 1998). New geochronological results from this area, obtained on phyllites, confirm the Miocene age, but again all dated samples contain only greenschist facies mineral assemblages (M. Bröcker & L. Franz, unpubl. data). An earlier HP episode is possibly indicated by high-Si phengite, however, the phengite populations comprise a considerable compositional range, similar to pervasively overprinted rocks from the overlying BGU. The existence of a basal unit on Tinos is questionable and unequivocal evidence for the timing of HP metamorphism in the lowermost sequences is not available. The Rb–Sr ages from the lowermost sequences on Tinos most likely indicate an upper time limit for greenschist facies overprinting of HP rocks that belong to the BGU.

The Almyropotamos unit (=basal unit) on Evvia consists of a thick marble sequence (*c.* 2000 m) overlain by clastic metasediments (*c.* 1500 m) interpreted as a metaflysch (Shaked *et al.*, 2000). According to these authors, the mineral assemblages of the metaflysch mainly include phengite, quartz, chlorite, albite, ±calcite, ±rare stilpnomelane and epidote. Glaucophane in the matrix was only found at one location, but occurs as inclusions in albite at other locations. Albite encloses relics of an earlier foliation. Relict glaucophane is replaced by biotite and chlorite. High-Si phengite occurs sporadically in the marbles. The mineral assemblage of schist intercalations in the marbles comprises chlorite, calcite, albite, phengite and quartz; glaucophane occurs as inclusion in albite porphyroblasts (Shaked *et al.*, 2000).

Ring & Reischmann (2002) dated two mica-rich phyllites with a greenschist facies mineral assemblage (including biotite, quartz and albite; no glaucophane relics) and interpreted the Rb–Sr phengite ages of 22.8 ± 0.2 and 22.8 ± 0.3 Ma as the time of HP metamorphism because the phengite is Si-rich (3.4–3.6) and unzoned. The lack of zonation was interpreted by these authors as an indication that the white mica was not affected by post-HP recrystallization. Possible age resetting was not taken into consideration. Is the absence of phengite zonation in a sample that does not contain the limiting assemblage unambiguous evidence for a lack of greenschist facies recrystallization? Is the geochronological record of high-Si phengite in an overprinted rock a reliable indicator for the timing of the HP event? In the light of the complexities described above, we think not. Our doubts are further nourished by additional geochronological data from the Almyropotamos unit reported by Ring & Layer (2003). A metaflysch sample with the assemblage phengite, biotite, chlorite, albite, calcite, graphite and quartz was dated by means of the ^{40}Ar–^{39}Ar method. White mica and biotite yielded poorly defined dates >30 Ma which were considered to reflect incomplete resetting of detrital phases and an excess argon component. ^{40}Ar–^{39}Ar ages of *c.* 33–31 Ma were also obtained on potassic white mica with high Si rims separated from the Almyropotamos marbles (Ring & Layer, 2003). These dates are not in accord with the 21–23 Ma age and were considered not to indicate the true time of the HP metamorphism because these ages do not agree with geochronological data previously reported from the basal units on Evvia, Samos, Tinos. But what is the geological significance of the older ages? Textural observations and mineral assemblages described by Shaked *et al.* (2000) and Ring & Reischmann (2002) indicate that the Almyropotamos unit was affected by HP metamorphism and a subsequent greenschist facies overprint. However, the samples dated are not well-preserved blueschist facies rocks and yielded a considerable range of ages, and thus do not provide unambiguous constraints for the timing of the HP event. These dates are compatible with the alternative interpretation that the Almyropotamos unit experienced pre-Miocene HP metamorphism and Miocene overprinting. If the fossil findings are correctly interpreted (Dubois & Bignot, 1979), the HP stage definitely must be younger than Eocene and therefore is different from the timing of HP metamorphism in the lower main unit of the ACCB (Shaked *et al.*, 2000).

In conclusion, the assumption that the basal units underwent HP metamorphism in the Miocene is not well substantiated. Geodynamic models using this hypothesis as a basic input parameter require further investigation. However, even if a Miocene age for the HP event can unambiguously be established, this does not necessarily require that these occurrences were ever in close proximity, it only indicates that these locations once belonged to the same metamorphic belt.

CONCLUSIONS

This study has shown that phengite dating of polymetamorphic rocks may be fraught with complexity, including the well-known problems related to mixing of different mica generations, inheritance, excess argon and retrograde disturbance of isotope systems. An important new finding of this study concerns the relationship between petrological and geochronological information provided by phengitic white mica and documents a problematic issue that has largely gone unnoticed. High-Si phengite commonly considered to have crystallized during HP conditions may instead record the time of a subsequent overprint at lower pressures, due to bulk-compositional constraints and poorly understood processes causing decoupling of baric and geochronological records. This observation has important implications for the interpretation of complex *P–T–t–d* paths and the understanding of geodynamic processes. For example, the correlation of high-Si phengite with ages of *c.* 24 Ma recognized on Tinos may lead to the erroneous conclusion that these rocks underwent Oligocene–Miocene HP metamorphism, which conflicts with the well-documented geochronological framework of the study area. The results of this study further emphasize the need for a careful analysis of the relationship between phengite chemistry and isotopic rejuvenation of rocks that were affected by multiple episodes of metamorphism and deformation.

ACKNOWLEDGEMENTS

This study was funded by the Deutsche Forschungsgemeinschaft (grant Br 1068/8-1), benefited from the financial support of this funding agency for the 'Zentrallaboratorium für Geochronologie' at Münster, and by the US NSF through grant EAR-0003568 to BRH. Thanks are due to H. Baier for laboratory assistance and U. Ring for patiently answering e-mails and providing a preprint of his Tectonics paper. Reviews by U. Ring, P. Dahl and an anonymous reviewer are much appreciated.

REFERENCES

Altherr, R., Schliestedt, M., Okrusch, M. *et al.*, 1979. Geochronology of high-pressure rocks on Sifnos (Cyclades, Greece). *Contributions to Mineralogy and Petrology*, **70,** 245–255.

Altherr, R., Kreuzer, H., Wendt, I. *et al.*, 1982. A Late Oligocene/Early Miocene high temperature belt in the Attic-Cycladic Crystalline Complex (SE Pelagonian, Greece). *Geologisches Jahrbuch*, **E 23,** 97–164.

Arnaud, N. O. & Kelley, S. P., 1995. Evidence for excess argon during high pressure metamorphism in the Dora Maira Massif (western Alps, Italy), using an ultra-violet laser ablation microprobe $^{40}Ar/^{39}Ar$ technique. *Contributions to Mineralogy and Petrology*, **121,** 1–11.

Avigad, D. & Garfunkel, Z., 1989. Low angle faults underneath and above a blueschist belt - Tinos Island, Cyclades, Greece. *Terra Nova*, **1,** 182–187.

Baldwin, S. L. & Lister, G. S., 1998. Thermochronology of the South Cyclades Shear Zone, Ios, Greece: effects of ductile shear in the argon partial retention zone. *Journal of Geophysical Research, Solid Earth*, **103,** 7315–7336.

Breeding, C. M., Ague, J. J., Bröcker, M. & Bolton, E. W., 2003. Blueschist preservation in a retrograded, high-pressure, low-temperature metamorphic terrane, Tinos, Greece: implications for fluid flow paths in subduction zones. *Geochemistry Geophysics, Geosystems*, **4,** 9001, doi:10.1029/2002GC000380.

Bröcker, M., 1990a. Die Blauschiefer-Grünschiefer-Assoziation der Insel Tinos (Kykladen, Griechenland) und ihre kontaktmetamorphe Überprägung. *Geotektonische Forschungen*, **74,** 1–107.

Bröcker, M., 1990b. Blueschist-to-greenschist transition in metabasites from Tinos Island (Cyclades, Greece): Compositional control or fluid infiltration. *Lithos*, **25,** 25–39.

Bröcker, M. & Enders, L., 1999. U-Pb zircon geochronology of unusual eclogite-facies rocks from Syros and Tinos (Cyclades, Greece). *Geological Magazine*, **136,** 111–118.

Bröcker, M. & Franz, L., 1998. Rb–Sr isotope studies on Tinos Island (Cyclades, Greece): additional time constraints for metamorphism, extent of infiltration-controlled overprinting and deformational activity. *Geological Magazine*, **135,** 369–382.

Bröcker, M. & Franz, L., 2000. Contact metamorphism on Tinos (Cyclades, Greece): the importance of tourmaline, timing of the thermal overprint and Sr isotope characteristics. *Mineralogy and Petrology*, **70,** 257–283.

Bröcker, M., Kreuzer, H., Matthews, A. & Okrusch, M., 1993. $^{40}Ar/^{39}Ar$ and oxygen isotope studies of polymetamorphism from Tinos Island, Cycladic blueschist belt. *Journal of Metamorphic Geology*, **11,** 223–240.

Dalrymple, G. B. & Duffield, W. A., 1988. High precision $^{40}Ar/^{39}Ar$ of Oligocene rhyolites from the Mogollon-Datil volcanic field using a continuous laser system. *Geophysical Research Letters*, **15,** 463–466.

Di Vincenzo, G., Ghiribelli, B., Giorgetti, G. & Palmeri, R., 2001. Evidence of a close link between petrology and isotope records: constraints from SEM, EMP, TEM and in situ $^{40}Ar–^{39}Ar$ laser analyses on multiple generations of white micas (Lanterman Range, Antarctica). *Earth and Planetary Science Letters*, **192,** 389–405.

Dubois, R. & Bignot, G., 1979. Presence d'un 'hard ground' nummulitique au de la série cretacée d'Almyropotamos (Eubee meridionale, Grece). *Paris, Academie des Sciences Comptes Rendus*, **289,** 993–995.

Dürr, S., 1986. Das Attisch-kykladische Kristallin. In: *Geologie von Griechenland* (ed. Jacobshagen, V.), pp. 116–148. Borntraeger, Berlin, Stuttgart.

El-Shazly, A. E., Bröcker, M., Hacker, B. R. & A. T. Calvert, 2001. Formation and exhumation of blueschists and eclogites from NE Oman: new constraints from Rb–Sr and $^{40}Ar/^{39}Ar$ dating. *Journal of Metamorphic Geology*, **19,** 233–248.

Giorgis, D., Cosca, M. & Li, S., 2000. Distribution and significance of extraneous argon in UHP eclogite (Sulu terrain, China): insights from in situ $^{40}Ar/^{39}Ar$ UV-laser ablation analysis. *Earth and Planetary Science Letters*, **181,** 605–615.

Guidotti, C. V. & Sassi, F. P., 1976. Muscovite as a petrogenetic indicator mineral in pelitic schists. *Neues Jahrbuch für Mineralogie, Abhandlungen*, **127,** 97–142.

Guidotti, C. V. & Sassi, F. P., 1986. Classification and correlation of metamorphic facies series by means of muscovite b_0 data from low-grade metapelites. *Neues Jahrbuch für Mineralogie, Abhandlungen*, **153,** 363–380.

Hacker, B. R. & Wang, Q. C., 1995. $^{40}Ar/^{39}Ar$ geochronology of ultrahigh-pressure metamorphism in central China. *Tectonics*, **14,** 994–1006.

Jolivet, L., Goffe, B., Monie, P., Truffert-Luxey, C., Patriat, M. & Bonneau, M., 1996. Miocene detachment in Crete and exhumation *P–T–t* paths of high-pressure metamorphic rocks. *Tectonics*, **15,** 1129–1153.

Katzir, Y., Matthews, A., Garfunkel, Z. & Schliestedt, M., 1996. The tectono-metamorphic evolution of a dismembered ophiolite (Tinos, Cyclades, Greece). *Geological Magazine*, **133,** 237–254.

Kühn, A., Glodny, J., Iden, K. & Austrheim, H., 2000. Retention of Precambrian Rb/Sr phlogopite ages through Caledonian eclogite facies metamorphism, Bergen Arc Complex, W-Norway. *Lithos*, **51,** 305–330.

Li, S., Wang, S., Chen, Y. *et al*., 1994. Excess argon in phengite from eclogite: evidence from dating of eclogite minerals by Sm-Nd, Rb–Sr and $^{40}Ar/^{39}Ar$ methods. *Chemical Geology (Isotope Geoscience Section)*, **112,** 343–350.

Ludwig, K. R., 1991. ISOPLOT; a plotting and regression program for radiogenic-isotope data; version 2.53. USGS Open File Report 91-0445.

Massonne, H. J., 1991. High-pressure, low-temperature metamorphism of pelitic and other protoliths based on experiments in the system K_2O-MgO-Al_2O_3-SiO_2-H_2O. Habilitation Thesis, Bochum, 172 pp.

Massonne, H. J. & Schreyer, W., 1987. Phengite geobarometry based on the limiting assemblage with K-feldspar, phlogopite, and quartz. *Contributions to Mineralogy and Petrology*, **96,** 212–224.

Massonne, H. J. & Schreyer, W., 1989. Stability field of the high-pressure assemblage talc + phengite and two new phengite barometers. *European Journal of Mineralogy*, **1,** 391–410.

Matthews, A., Lieberman, J., Avigad, D. & Garfunkel, Z., 1999. Fluid-rock interaction and thermal evolution during thrusting of an Alpine metamorphic complex (Tinos Island, Greece). *Contributions to Mineralogy and Petrology*, **135,** 212–224.

Maurel, O., Monié, P., Respaut, J. P., Leyreloup, A. F. & Maluski, H., 2003. Pre-metamorphic $^{40}Ar/^{39}Ar$ and U-Pb ages in HP metagranitoids from the Hercynian belt (France). *Chemical Geology*, **193,** 195–214.

Melidonis, N. G., 1980. The geological structure and mineral deposits of Tinos island (Cyclades, Greece). *The Geology of Greece*, **13,** 1–80.

Okrusch, M. & Bröcker, M., 1990. Eclogite facies rocks in the Cycladic blueschist belt, Greece: A review. *European Journal of Mineralogy*, **2,** 451–478.

Patzak, M., Okrusch, M. & Kreuzer, H., 1994. The Akrotiri unit on the island of Tinos, Cyclades, Greece: Witness to a lost terrane of Late Cretaceous age. *Neues Jahrbuch für Geologie und Paläontologie, Abhandlungen*, **194,** 211–252.

Ring, U. & Layer, P. W., 2003. High-pressure metamorphism in the Aegean, eastern Mediterranean: underplating and exhumation from the Late Cretaceous until the Miocene to Recent above the retreating Hellenic subduction zone. *Tectonics*, **22,** No. 3 10.1029/2001TC001350.

Ring, U. & Reischmann, T., 2002. The weak and superfast Cretan detachment, Greece: exhumation at subduction rates in extruding wedges. *Journal of the Geological Society London*, **159,** 225–228.

Ring, U., Layer, P. W. & Reischmann, T., 2001. Miocene high-pressure metamorphism in the Cyclades ande Crete, Aegean Sea, Greece: evidence for large-magnitude displacement on the Cretan detachment. *Geology*, **29,** 395–398.

Sassi, F. P., Guidotti, C. V., Rieder, M. & De Pieri, R., 1994. On the occurrence of metamorphic $2M_1$ phengites: some thoughts on polytypism and crystallization conditions of 3T phengites. *European Journal of Mineralogy*, **6,** 151–160.

Scaillet, S., 1998. K–Ar ($^{40}Ar/^{39}Ar$) geochronology of ultrahigh pressure rocks. In: *When Continents Collide: Geodynamics and Geochemistry of Ultrahigh-Pressure Rocks* (eds Hacker, B. R. & Liou, J. G.), pp. 161–201. Kluwer Academic Publishers, Dordrecht.

Shaked, Y., Avigad, D. & Garfunkel, Z., 2000. Alpine high-pressure metamorphism at the Almyropotamos Window (southern Evia, Greece). *Geological Magazine*, **137,** 367–380.

Sherlock, S. & Kelley, S., 2002. Excess argon evolution in HP-LT rocks: a UVLAMP study of phengite and K-free minerals, NW Turkey. *Chemical Geology*, **182,** 619–636.

Steiger, R. H. & Jäger, E., 1977. Subcommission on geochronology: convention on the use of decay constants in geo- and cosmochronology. *Earth and Planetary Science Letters*, **36,** 359–362.

Thomson, S. N., Stöckhert, B. & Brix, M. R., 1998. Thermochronology of the high-pressure metamorphic rocks of Crete, Greece: implications for the speed of tectonic process. *Geology*, **26,** 259–262.

Tomaschek, F., Kennedy, A. K., Villa, I. M., Lagos, M. & Ballhaus, C., 2003. Zircons from Syros, Cyclades, Greece – recrystallization and mobilization of zircon during high-pressure metamorphism. *Journal of Petrology*, **44,** 1977–2002.

Velde, B., 1967. Si^{+4} content of natural phengites. *Contributions to Mineralogy and Petrology*, **14,** 250–258.

Wijbrans, J. R. & McDougall, I., 1986. $^{40}Ar/^{39}Ar$ dating of white micas from an Alpine high-pressure metamorphic belt on Naxos (Greece): resetting of the argon isotopic system. *Contributions to Mineralogy and Petrology*, **93,** 187–194.

Wijbrans, J. R. & McDougall, I., 1988. Metamorphic evolution of the Attic Cycladic Metamorphic Belt on Naxos (Cyclades, Greece) utilizing $^{40}Ar/^{39}Ar$ age spectrum measurements. *Journal of Metamorphic Geology*, **6,** 571–594.

Wijbrans, J. R., Schliestedt, M. & York, D., 1990. Single grain argon laser probe dating of phengites from the blueschist to greenschist transition on Sifnos (Cyclades, Greece). *Contributions to Mineralogy and Petrology*, **104,** 582–593.

Received 24 August 2003; revision accepted 17 March 2004.